Archives of Materials Science and Engineering

Volume 126
Issue 2
April 2024
Pages 49-57

International Scientific Journal
published monthly by the
World Academy of Materials
and Manufacturing Engineering

DOI: 10.5604/01.3001.0054.6751

Impact of sintering time on structure and electrical properties of Pb-free BNT-BKT-SZ ceramics

S. Manotham [a], P. Butnoi [a,*], M. Khieokae [a], P. Paengchit [b], P. Prajansri [c]

[a] Department of Metallurgical Technology, Faculty of Technical Education, Rajamangala University of Technology Krungthep (RMUTK), Bangkok, Thailand
[b] Department of Industrial Technology, Faculty of Technical Education, Rajamangala University of Technology Krungthep (RMUTK), Bangkok, Thailand
[c] Physics Division, Faculty of Science and Technology, Rajamangala University of Technology Krungthep, Bangkok 10120, Thailand
* Corresponding e-mail address: pichitchai.b@mail.rmutk.ac.th
ORCID identifier: https://orcid.org/0000-0003-4353-7652 (P.B.)

ABSTRACT

Purpose: The work focuses on preparing and characterising BNT-based ceramics via a solid-state method. To investigate the phase, microstructure, and physical and electrical properties of BNT-based ceramics.

Design/methodology/approach: Lead-free piezoelectric bismuth sodium titanate – bismuth potassium titanate – stronsium zirconate (BNT-BKT-SZ) ceramics were fabricated by the solid-state reaction method. The effect of sintering temperature with soaking times of 2, 4, and 6 h at 1150°C on structural, microstructure, density, porosity, and electrical properties was examined. The phase formation of the ceramics was examined using X-ray diffraction (XRD). Scanning electron microscopy (SEM) (JEOL JSM5910LV) was employed to investigate ceramic microstructure. The bulk density and mechanical properties of the sample were measured using Archimedes' method, respectively. The electrical properties of ceramics, such as dielectrics, ferroelectrics, and piezoelectrics, were investigated.

Findings: XRD showed all samples had a single perovskite structure and no secondary phase. All sintered samples at different temperatures have a coexisting phase boundary between the rhombohedral phase and the tetragonal phase. The sintered ceramic at 1150°C with a soaking time of 4 h shows a maximum density of 5.89 g/cm3. In addition, the temperature at which the sintering process is carried out substantially impacts the electrical characteristics. Dielectric and electric field-induced strain (S_{max}) properties that sintered at 1150°C with a soaking time of 4 h exhibited the highest values of 4.489 and 0.39% (d_{33}* of 650 pm/V), respectively.

Research limitations/implications: The impact of the coercive field on the electrical breakdown characteristics of ceramics should be investigated further in the course of research that has to be carried out.

Practical implications: The characterisation confirmed the effects of sintering temperature on the physical, phase, microstructure, and electrical properties of BNT-based ceramics.

Originality/value: Such research demonstrates a suitable sintering temperature for producing BNT-BKT-SZ. The mechanical and electrical properties of a material are dependent on its sintering parameters. The ceramic system is suitable for piezoelectric and/or energy storage applications.

Keywords: Sintering times, Bismuth sodium titanate – bismuth potassium titanate – stronsium zirconate, Electrical properties, Piezoelectric

Reference to this paper should be given in the following way:

S. Manotham, P. Butnoi, M. Khieokae, P. Paengchit, P. Prajansri, Impact of sintering time on structure and electrical properties of Pb-free BNT-BKT-SZ ceramics, Archives of Materials Science and Engineering 126/2 (2024) 49-57. DOI: https://doi.org/10.5604/01.3001.0054.6751

PROPERTIES

1. Introduction

The piezoelectric ceramic material can instantly change the form of the energy it receives from a mechanical source into either electrical or mechanical form [1-4], and it has been widely used in many fields such as sensors, transducers, actuators, energy harvesters, and micro-electro-mechanical systems (MEMS) [3-11]. However, concerns have been expressed about the toxicity of lead, which is the main component of piezoelectric ceramics. Therefore, many scientists are now focusing on developing piezoelectric ceramics which do not contain lead [12,13]. Lead-free piezoelectric ceramics include many systems, for instance, $Bi_{0.5}Na_{0.5}TiO_3$ (BNT), $BaTiO_3$ (BT), and $Bi_{0.5}K_{0.5}TiO_3$ (BKT) [14-16]. BNT ceramic is an excellent choice for usage in piezoelectric applications due to its high Curie temperature (T_C 320°C), acceptable dielectric response, high piezoelectric response, and high electric energy density and hug strain under a high electric field because the polarizability of the Bi^{3+} ion is identical to the Pb^{2+} ion. Nevertheless, BNT presents a highly coercive field (E_c), making the poling process difficult [17-20]. In piezoelectric ceramics like PZT materials, both rhombohedral and tetragonal ferroelectric phases coexist, and the morphotropic phase boundary (MPB) plays a crucial role.

Many researchers have modified the piezoelectric capabilities of BNT ceramics using bismuth potassium titanate (BKT). Binary BNT-BKT systems exhibit a high piezoelectric coefficient close to the morphotropic phase boundary (MPB). At a BKT concentration of 15 to 20 mol%, the BNT-BKT at the MPB region demonstrated the coexistence of tetragonal and rhombohedral phases [21-23]. Improvements in the piezoelectric performance of BNT ceramics are promising but still do not compare with PZT materials. Other modifications to the BNT-BKT solid solution have been developed to increase its electrical properties. Afifi et al. [24] investigated BNT-BKT-$SrZrO_3$ film and the content of BKT in energy storage. They concluded that at a BKT concentration of 17.5%, the energy storage efficiency and recoverable energy storage density increased to 39.9% and 3.27 J/cm^2, respectively. Maqbool et al. [25] studied the effect of $SrZrO_3$ on the piezoelectric properties of $Bi_{0.5}Na_{0.5}TiO_3$ ceramic. By modifying BNT with $SrZrO_3$, they increased the piezoelectric performance of the material, achieving maximum residual polarization of 32 μC/cm^2 and piezoelectric constant 102 pC/N at 5% of SZ content. They also reported that BNT-SZ9 showed the maximum strain value induced by an electric field (S_{max} = 0.24%) corresponding to the normalized strain (d_{33}^* = 340 pm/V). Hao et al. [26] investigated the effect of $SrZrO_3$-doped BNKT20 ceramic on piezoelectric and ferroelectric properties. They concluded that with increasing SZ content, the ferroelectric rhombohedral and tetragonal phases in BNKT ceramic changed to the relaxor pseudocubic phases, leading to a field-induced strain improvement with a maximum value of ~0.39% and d_{33}^* ~488 pm/V. Several studies have modified BNT-based ceramics with BKT, KNN, BT, ST, and SZ, as well as ion doping. These additions improved the electrical properties of ceramics without a lead component. However, studies of the temperature and time of the sintering process are lacking. The BNT-BKT presented a morphotropic phase boundary (MPB), and SZ addition to BNT showed enhanced piezoelectric properties.

Therefore, such research focused on the influence of sintering time on the electrical properties of the 79($Bi_{0.5}Na_{0.5}TiO_3$)-20($Bi_{0.5}K_{0.5}TiO_3$)-1($SrZrO_3$); 79BNT-20BKT-1SZ ceramic during sintering at soaking times of 2, 4, and 6 h. Ceramics using the solid-state reaction process 79BNT-20BKT-1SZ were synthesised, and their structural, microstructural, dielectric, *P-E* hysteresis loop and piezoelectric characteristics were investigated and described in extensive detail.

2. Experimental

Na_2CO_3, TiO_2, Bi_2O_3, $SrCO_3$, K_2CO_3, and ZrO_2 were used as reagent grade raw materials to create the 0.79($Bi_{0.5}Na_{0.5}TiO_3$) + 0.20($Bi_{0.5}K_{0.5}TiO_3$) + 0.01($SrZrO_3$) ceramic using a solid-state reaction. The starting components were weighed using the appropriate chemical formula and then ball-milled using zirconia balls in ethanol for 24 h. The slurry was dried in an air oven at 100°C before

calcination at 900°C for two#hours. The powder was combined with a few drops of 4% PVA glue and then subjected to uniaxial pressing to form discs (diameter 10 mm and thickness 1.2 mm). The green pellets were sintered at 1150°C with soaking times of 2, 4, and 6 h.

X-ray diffraction (XRD) analysis verified the expected phase structure for these ceramics, and Archimedes' method was used to determine their density and porosity. The microstructure was inspected using a scanning electron microscope (SEM). For electrical characterisation, each sample was first polished and then coated on both sides with a silver paste before baking at 600°C for 30 min. The temperature dependence of the dielectric constant was determined from 30 to 500°C using an LCR meter. The ferroelectric and piezoelectric properties of the samples were measured using the Precision 10KV HVI-SC Workstation (Radiant Technologies, Inc.)

3. Results and discussion

Figure 1(a-c) displays the SEM images showing the surface morphology of the 79BNT-20BKT-1SZ ceramic. The micrographs revealed that the grains of all the samples had well-defined and consistent shapes with dense morphology. Fig. 1(d-f) shows the gain size distributions of the 79BNT-20BKT-1SZ ceramic. All the samples had a uniform normal distribution of grain sizes. It can be observed that thr average grain size of the sintered samples changed to 0.84 ± 0.21 μm, 1.02 ± 0.30 μm, and 1.05 ± 0.38 μm after soaking times of 2, 4, and 6 h, respectively (Tab. 1). Sample density increased at longer soaking times, reaching the maximum value of 5.89 g/cm^3 when the ceramic was sintered at 1150°C for 4 h. The density reduced#with increasing soaking time up to 6 h, caused by the loss of volatile alkali metal oxides due to exposure to higher temperatures [27]. Results showed that the porosity decreased with increasing soaking time to 6 h. The influence of grain size on porosity is probably the case because of the correlation between the irregularity of grains and the subsequent increase in porosity as particle size decreases [28-30].

Table 1.
Density and microstructural properties of the 79BNT-20BKT-1SZ ceramic

Dwell time, h	Density, g/cm^3	Porosity, %	Grain size, mm
2	5.62 ± 0.03	3.70 ± 0.12	0.84 ± 0.21
4	5.89 ± 0.02	0.97 ± 0.06	1.02 ± 0.30
6	5.75 ± 0.03	1.99 ± 0.63	1.05 ± 0.38

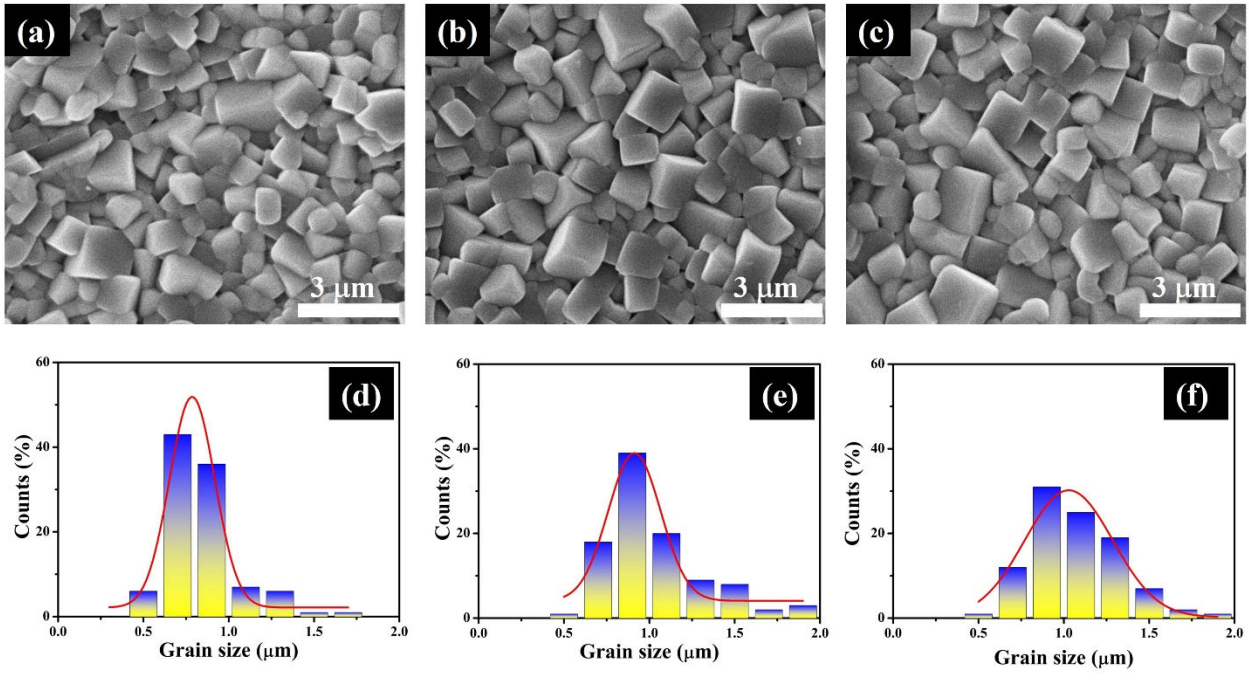

Fig. 1. SEM images and grain size distribution histograms of the 79BNT-20BKT-1SZ ceramic sintered at 1150°C with soaking times of (a),(d) 2 h; (b), (e) 4 h; and (c), (f) 6 h

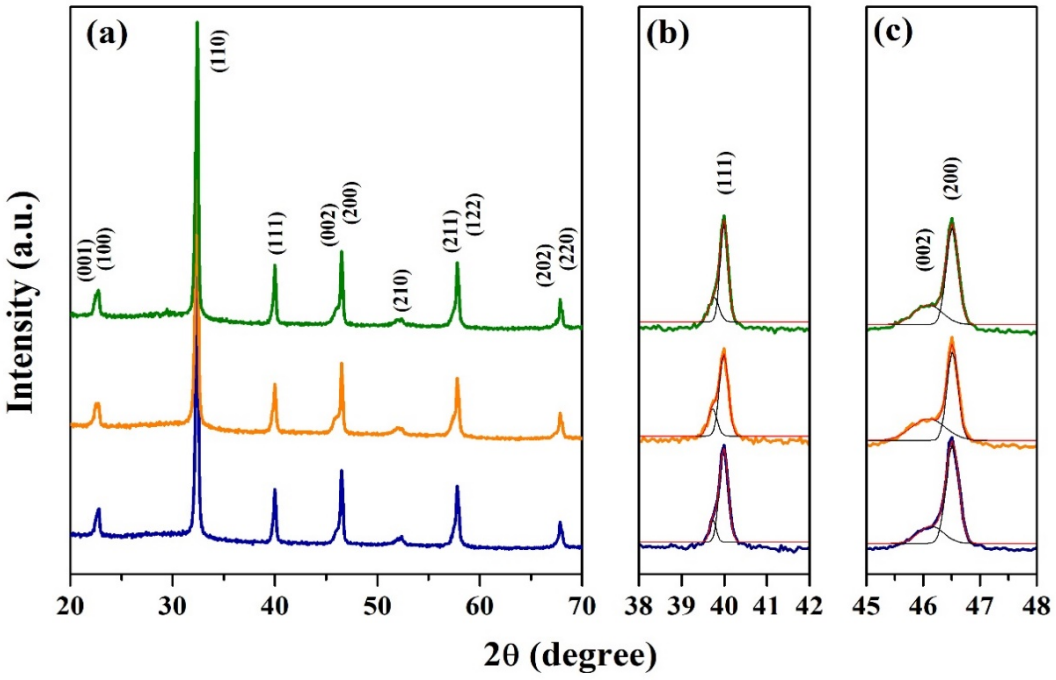

Fig. 2. (a) XRD patterns, (b) expanded magnification of (111) peaks, and (c) expanded magnification of the 79BNT-20BKT-1SZ ceramic sintered at various soaking times

Figure 2 (a) displays the XRD patterns of the 79BNT-20BKT-1SZ ceramic during the sintering process at soaking times of 2, 4, and 6 h. No secondary phases were detected in the studied range, indicating that all the ceramics were the pure perovskite phase and formed a homogeneous perovskite-structured solid solution. The XRD patterns of all the sintered samples showed a mixed rhombohedral and tetragonal structure. The splitting of the (111)/ (1$\bar{1}$1) peaks at around 40 degrees, indicating the rhombohedral phase, and the splitting of the (002)/(200) peaks at about 46 degrees, indicating the tetragonal phase, corroborated such a finding. The percentages of rhombohedral and tetragonal phases (%R and %T) were calculated by integrating the intensities of the XRD peaks, with results shown in Figure 3. The rhombohedral fraction increased in the sample sintered at four h, consistent with the apparent splitting of the (111)/(1$\bar{1}$1) peaks. On further increasing the soaking times to 6 h, the structure changed from a mixed phase to a tetragonal-rich phase and the (111) and (1$\bar{1}$1) peaks merged into a single (111) peak. The longer sintering process volatilized the alkali metal oxides, which resulted in the structural alterations discussed earlier [27].

The relationship between the temperature and the dielectric constant of the 79BNT-20BKT-1SZ ceramic sintered at 1150°C, with soaking times of 2, 4, and 6 h, was measured at frequencies ranging from 1 kHz to 1 MHz at 25 to 500°C, with results shown in Figure 4. All the samples displayed two types of dielectric anomalies at each tested frequency [31-33]. Below 200°C, a phenomenon known as depolarization (T_d) occurred in the dielectric constant, whereas the second (about 300°C) was the maximum dielectric constant (T_m). The dielectric properties as ε_{max}, T_d, and T_m values are listed in Table 21

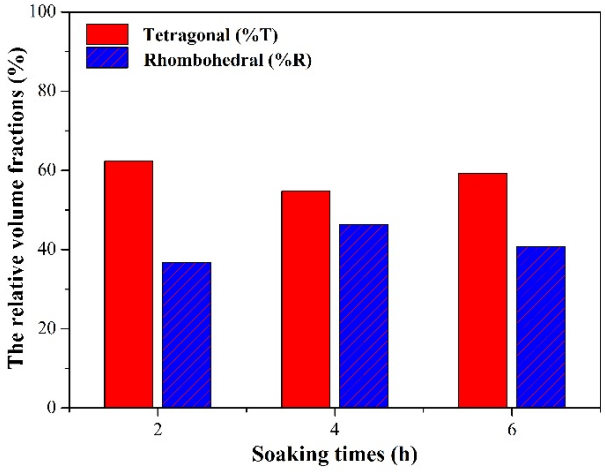

Fig. 3. Ratios of phases R and T of the 79BNT-20BKT-1SZ ceramic sintered at 1150°C with soaking times of 2, 4, and 6 h

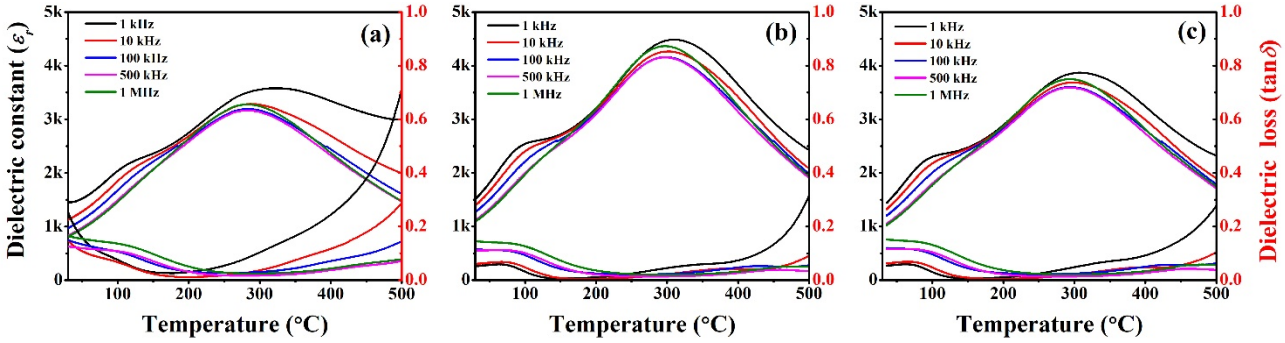

Fig. 4. Dependence of the dielectric constant (ε_r) and dielectric loss (tan δ) on temperature for the 79BNT-20BKT-1SZ ceramic sintered at 1150°C with soaking times of 2, 4, and 6 h

Table 2.
Dielectric properties of the 79BNT-20BKT-1SZ ceramic

Dwell time, h	ε_{max}, at 1 kHz	T_m, °C	T_d, °C
2	3566	305	112
4	4489	310	90
6	3870	308	88

The dielectric loss increased as the soaking time increased, while the dielectric constant increased with increasing sintering time. The sample sintered for four h showed the highest dielectric constant, with a maximum value of 4489.

Such an approach improved densification while simultaneously reducing porosity, ultimately leading to an improvement in the dielectric constant. In most cases, a higher density improves the dielectric properties of a material (thus reducing the porosity) by sintering at a high temperature. Alkathy et al. [34] reported that G. Arlt's theory explained the relationship between grain size and dielectric constant using the formula $Gd^{1/2}$(in the range of grain size 1-10 mm). The phase composition of the 4 h sample was extremely similar to the MPB area, which is another factor that contributed to this sample having the greatest dielectric constant. T_d values decreased with increasing dwell times. It may result from an ergodic relaxor (ER) phase ferroelectric order instability [35]. Obilor et al. [2] reported enhanced strain values when T_d is near room temperature.

Figure 5 shows the *P-E* hysteresis loops of the 79BNT-20BKT-1SZ ceramic sintered at different sintering times measured at 1 kHz under different electric fields. All *P-E* hysteresis loops in the sintered samples were asymmetric. Increased sintering time was accompanied by a rise in the coercive field (E_c) and the remnant polarization (P_r). The E_c and P_r values measured at 70 kV/cm (1 kHz) are given in Table 3.

Table 3.
Ferroelectric and piezoelectric properties of the 79BNT-20BKT-1SZ ceramic

Soaking time, h	P_r, μC/cm^2	P_s, μC/cm^2	E_c, kV/cm	Strain, %
2	4.3	25.7	8.7	0.31
4	22	37.6	16.5	0.39
6	6.6	32.0	13.9	0.36

The *P-E* hysteresis loops showed that the remnant polarization, coercive field, and shape were influenced by sintering times. The P_r and P_s values increased as sintering time increased from 2 h to 4 h, reaching a maximum of 22 mC/cm^2 and 37.6 mC/cm^2 at a soaking time of 4 h. The increase in P_r and P_s values as soaking time increased was due to the density increase [36], which had a beneficial impact on the ferroelectric properties of the material. Ceramics sintered at 1150°C with a soaking time of 6 h showed a slight decrease in P_r and P_s values because the low density that occurred during the sintering process impacted the value of the residual polarization [31,34]. Similar behaviour was seen in E_c, with the highest value of 16.5 kV/cm in the sample sintered for 4 h.

Figure 6 shows the bipolar strain-electric field (*S-E*) loops of the 79BNT-20BKT-1SZ ceramic recorded at room temperature (RT) in a 60 kV/cm electric field at 1 kHz. The maximum strain (S_{max}) is listed in Table 3. All samples showed a butterfly-shaped loop. The observed asymmetry in the *S-E* loops at 4 h and 6 h soaking times was due to the internal bias field with the motion of domains and domain walls [37,38]. The maximum strain of the sample sintered at 4 h was larger than the other samples.

The large strain value measured in this study was caused by a phase transition between the ergodic relaxor (ER) and ferroelectric (FE) phases (MPB region), which can occur in either direction. This transition was the cause of the

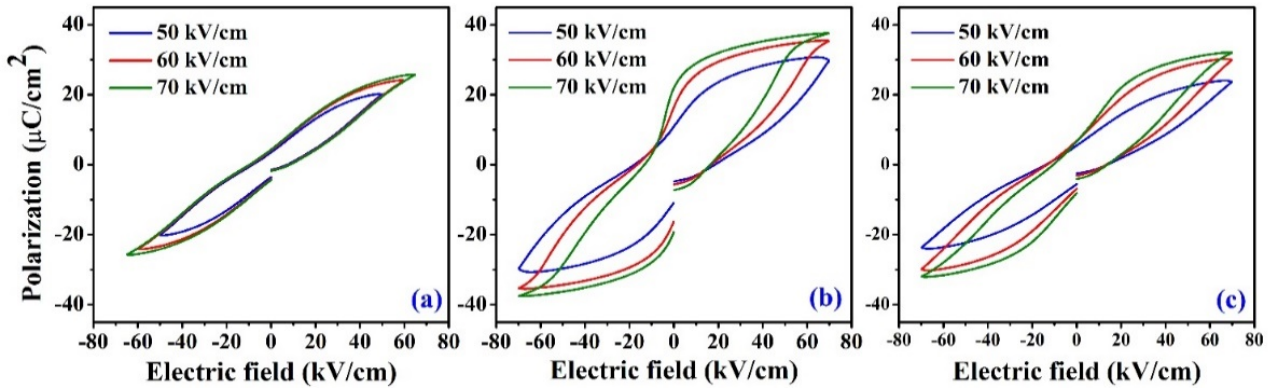

Fig. 5. *P-E* hysteresis loops of the 79BNT-20BKT-1SZ ceramic sintered at soaking times of (a) 2 h, (b) 4 h, and (c) 6 h

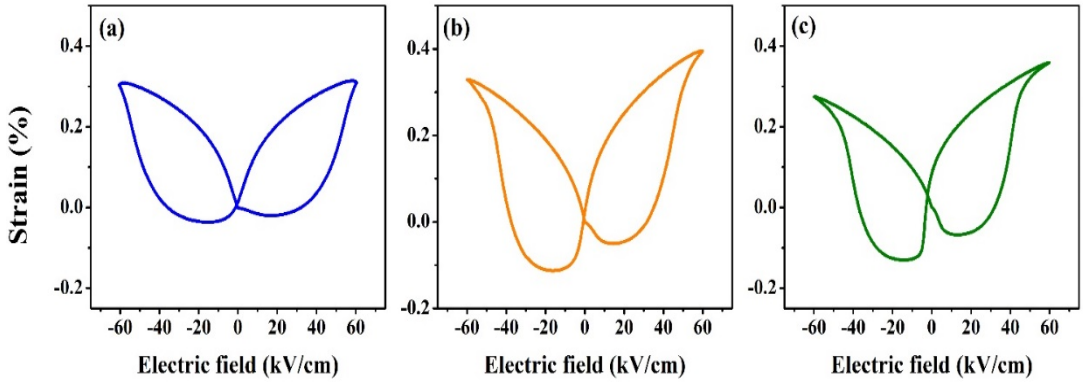

Fig. 6. Electric field-induced strain curves of the 79BNT-20BKT-1SZ ceramic sintered at soaking times of (a) 2 h, (b) 4 h, and (c) 6h

significant strain value [30, 39-42]. For many piezoceramics, including the ones under investigation, this can lead to a very large maximum apparent strain (S_{max}). An increase in the degree of ergodicity may be connected to the most significant strain and the lowest and/or disappearing negative strain value. This was demonstrated by pinching the *P-E* loop. As a result of such an event, the strain was maximally high, and the negative strain value was minimal or non-existent. The *P-E* loop exhibited an inward pinching motion, thereby demonstrating such a phenomenon.

4. Conclusions

The impact of sintering times on density, porosity, and electrical properties such as dielectric, ferroelectric, and piezoelectric were studied. A solid-state reaction technique was used to successfully manufacture the 79BNT-20BKT-1SZ ceramic. The XRD analysis results suggested that each ceramic had only one perovskite structure. Sintering under soaking time affected the dielectric, ferroelectric, and piezoelectric characteristics of such a ceramic. A suitable sintering time results in improved dielectric properties. The highest dielectric constant, which reached a maximum value of 4489, was found in the sample sintered with a dwell time of 4 h. Moreover, a large electric-induced strain (S_{max} = 0.39%) with high d_{33}^* (650 pm/V) was also reported for the same condition. The 79BNT-20BKT-1SZ ceramic sintered at 1150°C under 4 h soaking time showed promise as a lead-free ceramic for piezoelectric applications involving energy storage.

Research funding

The research was funded by the Department of Metallurgical Technology, Faculty of Technical Education, and Research Development Institute of Rajamangala University of Technology Krungthep (RMUTK), the National Research Council of Thailand (NRCT 662505011630 - 188716), Thailand.

Authors contribution

S.M. was involved in conceptualization, experiments, formal analysis, and writing – original draft – 35%. P.B. contributed to the investigation, characterization, writing – review and editing, supervision – 50%. M.K. was involved in experiments and analysis – 5%. P.P. was involved analysis, and P.P. was involved in electrical analysis. All authors discussed the results and contributed to the final manuscript.

References

[1] H. Ying, G. Ding, J. Zhao, J. Wang, Z. Liu, M. Zhou, J. Ye, Properties of PSN-PZT piezoelectric ceramic powder prepared by fast solid-phase reaction method, Materials Today Communications 35 (2023) 106086. DOI: https://doi.org/10.1016/j.mtcomm.2023.106086

[2] U. Obilor, C. Pascual-Gonzalez, S. Murakami, I.M. Reaney, A. Feteira, Study of the temperature dependence of the giant electric field-induced strain in Nb-doped BNT-BT-BKT piezoceramics, Materials Research Bulletin 97 (2018) 385-392. DOI: https://doi.org/10.1016/j.materresbull.2017.09.032

[3] S.H. Bakhy, M. Al-Waily, M.A. Al-Shammari, Analytical and numerical investigation of the free vibration of functionally graded materials sandwich beams, Archives of Materials Science and Engineering 110/2 (2021) 72-85. DOI: https://doi.org/10.5604/01.3001.0015.4314

[4] M.J. Jweeg, D.A. Alazawi, Q.H. Jebur, M. Al-Waily, N.J. Yasin, Hyperelastic modelling of rubber with multi-walled carbon nanotubes subjected to tensile loading, Archives of Materials Science and Engineering 114/2 (2022) 69-85. DOI: https://doi.org/10.5604/01.3001.0016.0027

[5] X. Huo, F. Wang, T. Zhang, M. Zhang, M. Guo, Adispersed polycrystalline phase boundary constructed in $CaZrO_3$ modified KNN based ceramics with both excellent piezoelectric properties and thermal stability, Ceramics International 49/10 (2023) 15751-15760. DOI: https://doi.org/10.1016/j.ceramint.2023.01.169

[6] H. Kuang, T. Liang, X. He, S. Wu, V. Oleg, D. Pang, Dielectric, ferroelectric, and piezoelectric properties of rare earth Sm-doped $0.94Bi_{0.5}Na_{0.5}TiO_3$-$0.06BaTiO_3$ lead-free ceramics, Journal of Alloys and Compounds 960 (2023) 170913. DOI: https://doi.org/10.1016/j.jallcom.2023.170913

[7] X. Li, S. Yue, S. Zhang, W. Long, P. Fang, F. Guo, Z. Xi, Z. Dai, Simultaneously enhanced piezoelectric response and Curie temperature in rhombohedral BS–PT ceramics by Zr doping, Materials Research Bulletin 165 (2023) 112307. DOI: https://doi.org/10.1016/j.materresbull.2023.112307

[8] S. Senthil Murugan, P. Vijayakumar, Identification of ultrasonic frequency for water mist generation using piezoelectric transducer. Archives of Materials Science and Engineering 83/2 (2017) 74-78. DOI: https://doi.org/10.5604/01.3001.0009.9170

[9] A. Mohaisen, T. Ntayeesh, An experimental and theoretical piezoelectric energy harvesting from a simply supported beam with moving mass, Archives of Materials Science and Engineering 123/1 (2023) 13-29. DOI: https://doi.org/10.5604/01.3001.0053.9754

[10] M. Jureczko, J. Filas, M. Mrówka, The application of piezoelectric materials to convert kinetic energy into electrical energy, Journal of Achievements in Materials and Manufacturing Engineering 121/2 (2023) 231-237. DOI: https://doi.org/10.5604/01.3001.0054.3211

[11] M. Chomiak, Reuse of polyester-glass laminate waste in polymer composites, Journal of Achievements in Materials and Manufacturing Engineering 107/2 (2021) 49-58. DOI: https://doi.org/10.5604/01.3001.0015.3583

[12] M. Habib, F. Akram, A. Rahman, P. Ahmad, M.J. Iqbal, Q. Liu, A. Zeb, D. Zhang, Defects dipoles control strategy for temperature-insensitive piezoelectricity in the lead-free $BiFeO_3$-$BaTiO_3$ ceramics, Materials Chemistry and Physics 287 (2022) 126326. DOI: https://doi.org/10.1016/j.matchemphys.2022.126326

[13] M. Mesrar, A. Elbasset, N.-S. Echatoui, F. Abdi, T. Lamcharfi, Microstructural and high-temperature dielectric, piezoelectric and complex impedance spectroscopic properties of $K_{0.5}Bi_{0.5}TiO_3$ modified NBT-BT lead-free ferroelectric ceramics, Heliyon 9/4 (2023) e14761. DOI: https://doi.org/10.1016/j.heliyon.2023.e14761

[14] X. Wang, Y. Huan, S. Ji, Y. Zhu, T. Wei, Z. Cheng, Ultra-high piezoelectric performance by rational tuning of heterovalent-ion doping in lead-free piezoelectric ceramics, Nano Energy 101 (2022) 107580. DOI: https://doi.org/10.1016/j.nanoen.2022.107580

[15] M. Habib, F. Akram, P. Ahmad, F.F. Al-Harbi, I. Ud Din, Q. Iqbal, T. Ahmed, S.A. Khan, A. Hussain, T.-K. Song, M.-H. Kim, S. Lee, Donor multiple effects on the ferroelectric and piezoelectric performance of lead-free $BiFeO_3$-$BaTiO_3$ ceramics, Materials Letters 315 (2022) 131950. DOI: https://doi.org/10.1016/j.matlet.2022.131950

[16] M. Ito, M. Hagiwara, S. Fujihara, Ferroelectric and piezoelectric properties of $(Bi_{1/2}K_{1/2})(Zr_xTi_{1-x})O_3$ lead-

free ceramics, Materials Letters 271 (2020) 127776. DOI: https://doi.org/10.1016/j.matlet.2020.127776

[17] A. Deng, J. Wu, Enhanced strain and electrostrictive properties in lead-free BNT-based ceramics via rare earth doping, Journal of Materiomics 8/2 (2022) 401-407. DOI: https://doi.org/10.1016/j.jmat.2021.08.002

[18] A. Syed, A. Sohail Khan, A. Ullah, M.R. Sarker, M. Tahir Khan, A. Ali, H. Ur Rashid, V. Tirth, A. Zaman, Enhancement of the phase, optical and dielectric studies of $Bi_{0.5}Na_{0.5}TiO_3$ (BNT) based structure ceramics, Journal of Saudi Chemical Society 27/2 (2023) 101617. DOI: https://doi.org/10.1016/j.jscs.2023.101617

[19] W. Kang, Z. Zheng, Y. Li, R. Zhao, Enhanced dielectric, piezoelectric properties and strengthened relaxor behavior in K-modified $Na_{0.5}Bi_{0.5}TiO_3$ lead-free ceramics, Ceramics International 46/15 (2020) 24091-24096. DOI: https://doi.org/10.1016/j.ceramint.2020.06.187

[20] Q. Wei, M. Zhu, M. Zheng, Y. Hou, High piezoelectric properties above 150°C in $(Bi_{0.5}Na_{0.5})TiO_3$-Based lead-free piezoelectric ceramics, Materials Chemistry and Physics 249 (2020) 122966. DOI: https://doi.org/10.1016/j.matchemphys.2020.122966

[21] X. Wang, H. Gao, X. Hao, X. Lou, Enhanced piezoelectric, electrocaloric and energy storage properties at high temperature in lead-free $Bi_{0.5}(Na_{1-x}K_x)_{0.5}TiO_3$ ceramics, Ceramics International 45/4 (2019) 4274-4282. DOI: https://doi.org/10.1016/j.ceramint.2018.11.100

[22] R.I. Mahdi, N.J. Al-Bahnam, A.I. Abbo, J.K. Hmood, W.H.A. Majid, Optimization of sintering temperature for the enhancement of pyroelectric properties of lead-free $0.88(Na_{0.5}Bi_{0.5})TiO_3–0.084(K_{0.5}Bi_{0.5})TiO_3–0.036BaTiO_3$ piezoelectric ceramics, Journal of Alloys and Compounds 688/A (2016) 77-87. DOI: https://doi.org/10.1016/j.jallcom.2016.06.290

[23] P. Fan, Y. Zhang, J. Huang, W. Hu, D. Huang, Z. Liu, B. Xie, X. Li, J. Xiao, H. Zhang, Constrained sintering and electrical properties of BNT–BKT lead-free piezoceramic thick films, Ceramics International 42/2/A (2016) 2534-2541. DOI: https://doi.org/10.1016/j.ceramint.2015.10.055

[24] M. Afifi, A.O. Turky, M. Rasly, M.M. Rashad, J.A. Turner, Field-induced polarization response and energy storage behavior of lead-free BNT-BKT-SZ films, Ceramics International 46/16/A (2020) 26061-26068. DOI: https://doi.org/10.1016/j.ceramint.2020.07.099

[25] A. Maqbool, A. Hussain, J.U. Rahman, J.K. Park, T.G. Park, J.S. Song, M.H. Kim, Ferroelectric and piezoelectric properties of $SrZrO_3$-modified $Bi_{0.5}Na_{0.5}TiO_3$ lead-free ceramics, Transactions of Nonferrous Metals Society of China 24/S1 (2014) s146-s151. DOI: https://doi.org/10.1016/S1003-6326(14)63302-1

[26] J. Hao, Z. Xu, R. Chu, W. Li, J. Du, Large electric-field-induced strain in $SrZrO_3$ modified $Bi_{0.5}(Na_{0.80}K_{0.20})_{0.5}TiO_3$ lead-free electromechanical ceramics with fatigue-resistant behavior, Journal of Alloys and Compounds 647 (2015) 857-865. DOI: https://doi.org/10.1016/j.jallcom.2015.06.151

[27] Y.-R. Zhang, J.-F. Li, B.-P. Zhang, Enhancing Electrical Properties in NBT–KBT Lead-Free Piezoelectric Ceramics by Optimizing Sintering Temperature, Journal of the American Ceramic Society 91/8 (2008) 2716-2719. DOI: https://doi.org/10.1111/j.1551-2916.2008.02469.x

[28] S. Zhang, W. Liu, G. Granata, Effects of grain size gradation on the porosity of packed heap leach beds, Hydrometallurgy 179 (2018) 238-244. DOI: https://doi.org/10.1016/j.hydromet.2018.06.014

[29] N.A. Ogolo, O.G. Akinboro, J.E. Inam, F.E. Akpokere, M.O. Onyekonwu, Effect of Grain Size on Porosity Revisited, Proceedings of the SPE Nigeria Annual International Conference and Exhibition, Lagos, Nigeria, 2015, SPE-178296-MS. DOI: https://doi.org/10.2118/178296-MS

[30] P. Butnoi, S. Manotham, T. Tunkasiri, Effect of sintering temperature on mechanical and electrical properties of lead-free $Bi_{0.5}(Na_{0.4}K_{0.1})Ti_{0.98}Zr_{0.02}O_3$ piezoelectric ceramics, Key Engineering Materials 798 (2019) 212-217. DOI: https://doi.org/10.4028/www.scientific.net/KEM.798.212

[31] A. Hussain, J.U. Rahman, A. Zaman, R.A. Malik, J.S. Kim, T.K. Song, W.J. Kim, M.H. Kim, Field-induced strain and polarization response in lead-free $Bi_{1/2}(Na_{0.80}K_{0.20})_{1/2}TiO_3–SrZrO_3$ ceramics, Materials Chemistry and Physics 143/3 (2014) 1282-1288. DOI: https://doi.org/10.1016/j.matchemphys.2013.11.035

[32] S. Manotham, P. Butnoi, N. Lertcumfu, P. Jaita, Effects of sintering temperatures on structural, electrical and mechanical properties of BNKT piezoelectric ceramics, Key Engineering Materials 777 (2018) 60-64. DOI: https://doi.org/10.4028/www.scientific.net/KEM.777.60

[33] S. Manotham, P. Butnoi, P. Jaita, N. Kumar, K. Chokethawai, G. Rujijanagul, D.P. Cann, Large electric field-induced strain and large improvement in energy density of bismuth sodium potassium titanate-based piezoelectric ceramics, Journal of Alloys and Compounds 739 (2018) 457-467. DOI: https://doi.org/10.1016/j.jallcom.2017.12.175

[34] M.S. Alkathy, A. Hezam, K.S.D. Manoja, J. Wang, C. Cheng, K. Byrappa, K.C.J. Raju, Effect of sintering temperature on structural, electrical, and ferroelectric properties of lanthanum and sodium co-substituted barium titanate ceramics, Journal of Alloys and Compounds 762 (2018) 49-61. DOI: https://doi.org/10.1016/j.jallcom.2018.05.138

[35] Q. Zhou, C. Zhou, H. Yang, C. Yuan, W. Li, Dielectric properties and depolarization temperature of $Bi_{0.5}(Na, K)_{0.5}TiO_3$–$BiFeO_3$ lead-free ceramics, Physica B: Condensed Matter 405/2 (2010) 613-618. DOI: https://doi.org/https://doi.org/10.1016/j.physb.2009.09.075

[36] M. Reda, S.I. El-Dek, M.M. Arman, Improvement of ferroelectric properties via Zr doping in barium titanate nanoparticles, Journal of Materials Science: Materials in Electronics 33 (2022) 16753-16776. DOI: https://doi.org/10.1007/s10854-022-08541-x

[37] X. Tian, Z. Wu, Y. Jia, J. Chen, R.K. Zheng, Y. Zhang, H. Luo, Remanent-polarization-induced enhancement of photoluminescence in Pr^{3+}-doped lead-free ferroelectric $(Bi_{0.5}Na_{0.5})TiO_3$ ceramic, Applied Physics Letters 102/4 (2013) 042907. DOI: https://doi.org/10.1063/1.4790290

[38] L. Liu, D. Shi, M. Knapp, H. Ehrenberg, L. Fang, J. Chen, Large strain response based on relaxor-antiferroelectric coherence in $Bi_{0.5}Na_{0.5}TiO_3$–$SrTiO_3$–$(K_{0.5}Na_{0.5})NbO_3$ solid solutions, Journal of Applied Physics 116 (2014) 184104. DOI: https://doi.org/10.1063/1.4901549

[39] J. Suchanicz, K. Kluczewska-Chmielarz, D. Sitko, G. Jagło, Electrical transport in lead-free $Na_{0.5}Bi_{0.5}TiO_3$ ceramics, Journal of Advanced Ceramics 10 (2021) 152-165. DOI: https://doi.org/10.1007/s40145-020-0430-5

[40] C. He, X. Bai, J. Wang, Y. Liu, Y. Lu, X. Liu, Y. Xiang, Z. Xu, Y. Chen, Structural, Piezoelectric and Dielectric Properties of $K_{0.4}Na_{0.6}NbO_3$-$Bi_{0.5}Li_{0.5}ZrO_3$-$CaZrO_3$ Ternary Lead-Free Piezoelectric Ceramics, Journal of Electronic Materials 49 (2020) 4364-4371. DOI: https://doi.org/10.1007/s11664-020-08174-y

[41] N. Truong-Tho, D. Le Vuong, Study on the strain behavior and piezoelectric properties of lead-free $Bi_{0.5}(Na_{0.8}K_{0.2})_{0.5}TiO_3$ ceramics modified with Sn^{4+} ions, Journal of Materials Science: Materials in Electronics 32 (2021) 16601-16611. DOI: https://doi.org/10.1007/s10854-021-06215-8

[42] S. Manotham, P. Butnoi, P. Jaita, S. Pinitsoontorn, D. Sweatman, S. Eitssayeam, K. Pengpat, G. Rujijanagul, Dielectric and Magnetic Properties of $Ba(Fe_{1/2}Ta_{1/2})O_3$-$BiFeO_3$ Ceramics, Journal of Electronic Materials 45 (2016) 5948-5955. DOI: https://doi.org/10.1007/s11664-016-4811-z